

Introduction

A dynamical system is a system illustrated by a specific set of values that uniquely determines the state and its behavior, which is governed by predefined rules. It is generally characterized by continuous timelines or discrete time steps. The systems that deal with discrete time steps are called discrete dynamical systems, which are usually described by the difference equations. These discrete-time systems are characterized by mathematical equations or rules that determine the future state of the system based on its current and previous states. The subject discrete dynamical system has made significant contributions to understand the nonlinear phenomena present in the system. It has applications in various scientific fields, including physics, biology, ecology, economics, etc., and provides a powerful framework for studying the modeling of complex phenomena.

In nature, the term population refers to the members of a single species or a community of species that can interact with each other. The population dynamics is essentially the study of the changes in numbers through time. The factors affecting the changes are the physiology of the individuals, environmental resources, and interactions between species of the same or different types. There exists an intrinsic difficulty in analyzing the factors influencing the growth and death of a species. Even for each of the simple cases of population, we can have different modeling approaches and strategies. Population modeling allows the quantification of biological interactions and proposes different modeling strategies with various presumptions to characterize certain population traits. From the mathematical perspective, there are essentially two main modeling approaches in population dynamics. The first one is the continuous-time approach using methods from ordinary differential equations, and the other one is the discrete-time approach, which is more closely associated with the difference equations. Both approaches have been extensively used to study the qualitative theory of dynamical systems. In the continuous-time method, the number of individuals within a population changes continuously throughout time. This modeling framework may be used to describe many kinds of biotic interspecific as well as their interactions with the environment. Further, with the development of the theory of modeling, the ideas of the carrying capacity of the ecosystem and the population growth rate are crucial to modern ecology. The assumptions of the theoretical models determine how beneficial population dynamics is for prediction and resource management.

The discrete population model of a single species emerged from the well-known work by May [May, 1976] that was published in Nature many years ago. The literature has several single-species models that can be used to simulate diverse biological populations. Two seminal works on discrete population modeling were provided by Ricker [Ricker, 1954]; Beverton and Halt [Beverton, 1957]. The single-species Ricker model was proposed mathematically to represent the stock and fisheries, which is given as follows:

$$x_{n+1} = x_n e^{\mu(1 - \frac{x_n}{K})},$$

where μ represents the intrinsic growth rate, and K denotes the maximum carrying capacity of the environment. The term $e^{\mu(1 - \frac{x_n}{K})}$ represents the survival function between the species at the n^{th} generation. Here, x_{n+1} and x_n represents the species population at the $(n+1)^{th}$ and n^{th} generation respectively. The Ricker population model can be written equivalently as

$$x_{n+1} = \lambda x_n e^{-\delta x_n} \equiv f(x_n), \tag{1.1}$$

where $\lambda = e^\mu$ and $\delta = \frac{\mu}{K}$. The model assumes that all the individuals have an equal influence on the size of the population and the growth rate of species is density-independent. Ricker population model is a widely studied model; along with its classical form, various other forms of the Ricker map have also been reviewed, for example, the k periodic Ricker map [Elaydi and Sacker, 2010], the Ricker map with an almost periodic coefficient [Sacker and Sell, 2017], etc. The Ricker model contains two parameters that make this model relatively inflexible. Consequently, it is unable to provide an appropriate fit for the stock-recruitment curve of the field data. To overcome this difficulty, a parameter $\gamma > 0$ is introduced as an additional parameter to the existing Ricker model to increase its flexibility. The modified map is named as *gamma Ricker map*, which is given as

$$x_{n+1} = \lambda x_n^\gamma e^{-\delta x_n},$$

where γ is the cooperation or Allee effect parameter. The three-parameter gamma Ricker map is more flexible and accurately fits the stock-recruitment curve to the field data. The dynamics of the gamma Ricker map have been discussed by researchers in many different contexts [Liz, 2018; Rocha and Taha, 2020]. In [Liz, 2018], the author describes that the gamma Ricker model represents a population whose per-capita growth rate shows both positive and negative density dependence for a certain range of parameters. In [Rocha and Taha, 2020], the dynamics, bifurcation, and the Allee effect bifurcation, which is different from pitchfork bifurcation, are discussed for the gamma Ricker map. When the per-capita birth or the growth function of the gamma Ricker map is characterized by the Holling type II functional response, which is given as

$$b(x_n) = \frac{cx_n}{x_n + \beta}, \quad (1.2)$$

where $c > 0$ measures the maximum growth rate, and the ratio c/β represents the relative growth rate as the population size is small, then the modified map with Holling type II function as a growth function is given as follows

$$x_{n+1} = r \frac{x_n^\gamma}{x_n + \beta} e^{-\delta x_n}, \quad (1.3)$$

where $r = \lambda c^\gamma$. The particular case of Eq.(1.3) at $\gamma = 1$ is known as the Homographic Ricker map $H(x)$, which is given as follows

$$x_{n+1} = r \frac{x_n}{x_n + \beta} e^{-\delta x_n} \equiv H(x_n). \quad (1.4)$$

The dynamics of the flexible three-parameter Homographic Ricker population model have been discussed by L. Rocha in [Rocha et al., 2020]. The nonlinear dynamics and bifurcation structure of the γ Ricker population model with a Holling type II per-capita birth function, with $\gamma = 2$, is discussed in [Rocha and Taha, 2021]. Moreover, a generalized r -Lambert W function is defined on 3D parameter space to determine the existence and variation of the number of non-zero fixed points of the Homographic 2 Ricker map. Further, the general case of a one-dimensional γ -Ricker map with Holling type II per-capita birth function is discussed in [Rocha and Taha, 2023].

The thermodynamic and mechanical systems introduce several innovative approaches for dealing with complex problems, many of which are efficient, though they differ from the standard ones. One of them is Tsallis's statistical mechanics [Tsallis, 1988], which motivates the q deformation of nonlinear maps. The deformation of a nonlinear map is obtained by introducing a parameter q in the original map such that the original map can be recovered when q approaches to 1. There are many deformations defined in the different contexts of mathematical problems; therefore, the deformation is not unique. In [Jaganathan and Sinha, 2005], the deformation of a real number is defined as

$$[x]_\varepsilon = \frac{x}{1 + \varepsilon(1 - x)}, \quad (1.5)$$

where $x \in \mathbb{R} \setminus \{1 + \frac{1}{\varepsilon}\}$ and $\varepsilon \in (-1, \infty)$. The number $[x]_\varepsilon \rightarrow x$, whenever $\varepsilon \rightarrow 0$. Clearly, the $[x]_\varepsilon$ is a homeomorphism which is increasing whenever $x \neq (1 + \frac{1}{\varepsilon})$. The deformed function f is obtained by the composition of f with $[\cdot]_\varepsilon$.

To stabilize the nonlinear system, one can use the deformation scheme and then study the complexity of the deformed system when the deformed parameter approaches the limiting case. The deformed map attracted several researchers over a long period because of the emergence of quantum group structures in many physical problems. Many applications in physical systems are shown by the creation of several q -deformed models as described in [Jaganathan and Sinha, 2005; Patidar et al., 2010; Iyengar and Balakrishnan, 2014; Cánovas and Muñoz-Guillermo, 2020; Gupta and Chandramouli, 2021, 2023]. For example, in the applied field of image processing where chaotic maps are used to generate pseudo-random numbers. Many other applications can be found in the area of watermarking process [Behnia et al., 2017], security systems, etc. The q deformation also plays a vital role in modeling various biological systems to understand their dynamics. In [Iyengar and Balakrishnan, 2014], the concept of q deformation is applied to improve and modify a tritrophic population model to understand the defoliation of coniferous Larch trees.

The Allee effect in population dynamics is known as the coexistence of attractors, and it has been extensively researched for unimodal maps [Sacker, 2007; Schreiber, 2017]. Most of the one-dimensional discrete dynamical system undergoes a period-doubling route to chaos. Nevertheless, a slight modification in the original system makes it possible to follow a sequence of reverse period-doubling bifurcation [Bier and Bountis, 1984; Ambika and Sujatha, 2000]. This kind of situation leads to controlling the chaos. In this process, a bubble-like structure is formed, which helps to keep the system in an equilibrium position. Ricker [Ricker, 1954] suggested the possibility of an increase in the population size in response to an increase in the death rate for the density-dependent population growth model. Abrams [Abrams, 2009] surveys this phenomenon, particularly for the one-dimensional population models with non-overlapping population and terms such as *hydra effect* or *hydra paradox*. E. Liz discussed the hydra effect and bubble formation in the population models with constant harvesting in [Liz, 2010; Liz and Hilker, 2012, 2014], and references therein.

Bifurcation analysis is a crucial tool in discrete dynamical systems, enabling the examination and prediction of a system's long-term behavior. It explores the qualitative change in the system's behavior with the change in the system's parameters. Some important bifurcations of the discrete systems are transcritical, fold (saddle-node), flip (period-doubling), and Neimark-Sacker bifurcation. These bifurcations describe the important transitions in the dynamics of a system and frequently represent a change from one qualitative state to another. In some systems, the analysis is quite simple, providing clear insights into the stability and behavior of the periodic points. In contrast, in some systems, these bifurcations result in richer and more complicated dynamics, potentially leading to chaotic behavior.

In transcritical bifurcation, as the control parameter crosses its critical value, the stability of the fixed point exchanges, i.e., a stable fixed point becomes unstable, and an unstable fixed point becomes stable. This exchange of stability happens when the fixed points intersect and pass through each other, resulting in changing the roles of the fixed point. This usually occurs in population dynamics, where the system undergoes a smooth exchange of stability between two states. In fold (saddle-node) bifurcation, the two fixed points (one stable and one unstable) merge into a single point and then disappear as the control parameter crosses its critical value. This bifurcation is important because it represents a situation where the system suddenly loses or gains stability as the parameter changes. In flip (period-doubling) bifurcation, the fixed point becomes unstable, and it leads to the generation of the stable period two-point as the control parameter crosses its critical value. This bifurcation can create cascades of period doubling, which lead to chaotic dynamics. In the higher dimensional systems, this bifurcation can lead to more intricate patterns of chaos. The

Neimark-Sacker (Hopf) bifurcation occurs when a fixed point of a two-dimensional discrete system loses stability, leading to the birth of a closed invariant curve. This explains how the system takes the transition from regular to more complicated behavior. It occurs when the eigenvalues λ_1 and λ_2 of the Jacobian matrix of the map are the complex conjugates having unit modulus and cross the unit circle in the complex plane as the control parameter crosses its critical value.

In the first part of the thesis, we consider the q -deformation scheme presented in [Jaganathan and Sinha, 2005], which is inspired from Tsalli's q exponential function applied on the one-dimensional maps: Ricker map and Homographic Ricker map and obtain the q -deformed maps. The aim of the work is to investigate the nonlinear dynamics of the q -Ricker map and q -Homographic map.

In Chapter 2, we apply the deformation scheme given by Eq.(1.5) to the Ricker map $f(x)$ and obtain the q -deformed Ricker map $R_\varepsilon(x)$, defined as

$$R_\varepsilon(x) = \frac{\lambda x e^{-\beta x}}{1 + \varepsilon(1 - \lambda x e^{-\beta x})}. \quad (1.6)$$

We discuss the dynamics of the q -Ricker map in the following parameter region

$$\Sigma = \left\{ (\varepsilon, \beta, \lambda) : \varepsilon \in (-1, \infty) \setminus \{0\}, \beta > \frac{\lambda_0}{e(1+1/\varepsilon)}, e\beta_0 \left(1 + \frac{1}{\varepsilon}\right) > \lambda > 0 \right\}, \quad (1.7)$$

for a fixed λ_0 and β_0 .

We analyze the basic nonlinear dynamics, bifurcation structure, and topological entropy of the q -Ricker map. The topological entropy of the q -Ricker map is calculated with the help of the algorithm proposed in [Block et al., 1989]. The negative Schwarzian derivative and positive topological entropy confirm the presence of Li-Yorke chaos in the q -Ricker map. Further, we observe that the map has some parameter regions where the chaos is not physically observable. The q -Ricker map proclaims many remarkable phenomena in the one-dimensional dynamics, such as the presence of coexisting attractors, physically non-observable chaos, hydra paradox, bubbling effect, and extinction phenomena. The bifurcation theory of the dynamical systems allows us to obtain the fold and flip bifurcation curves associated with the trivial and non-trivial fixed points of the q -Ricker map. The intersection of the fold and flip bifurcation curves in the $\varepsilon - \lambda$ plane gives a singular point of co-dimension greater than two, and the singularity merges with its associated cusp point. Let $\Lambda_{(1)}^1$ and Λ_1^1 represents the fold and flip bifurcation curves corresponding to $x^* = 0$, while $\Lambda_{(1)}^2$ and Λ_1^2 are corresponding to the other positive fixed point. The intersection of fold and flip bifurcation curves leads to the following propositions.

Proposition 1.0.1. *Let $R_\varepsilon(x)$ be the q -Ricker map. In the $(X^*, \Delta_{\varepsilon, \lambda})$ space with $\beta = 2$ as a constant,*

(i) *then we have*

$$\Lambda_{(1)}^1 \cap \Lambda_{(1)}^2 \cap \Lambda_1^1 = \{(-1, 0)\}.$$

(ii) *Further, the singular line corresponding to the fixed point $x^* = 0$ of the map $R_\varepsilon(x)$ is the set*

$$\tilde{\Lambda} = \{(\lambda, \varepsilon, \beta_0) \in \Sigma : \lambda \rightarrow 0, \varepsilon \rightarrow -1\}.$$

The merging of a saddle point into its corresponding cusp point is also a result of tangency between the bifurcation curves. In a specific scenario, when the map has a multiplier equal to 1, the saddle point is just the tangent point between the two fold bifurcation curves. This above result leads to the following proposition:

Proposition 1.0.2. *Let $R_\varepsilon(x)$ be the q -Ricker map. In the $(X^*, \Delta_{\varepsilon, \lambda})$, with parameter $\beta = \beta_0$, the singular point $(\beta_0, 1 + \beta_0)$ is a saddle point which merges with its associated cusp point.*

The q -Ricker map reveals the phenomena of bubbling and the Hydra paradox with respect to the change in the deformed parameter ε . However, these effects manifest within a specific range of deformed parameters. In conclusion, excessive deformation can lead to system instability, but adequate deformation can maintain system stability. By employing the bubbling process, one can determine the deformation parameter that ensures the system remains in a stable state. The outcomes of Chapter 2 are based on the following article.

Aishwaraya, Gupta, D., and Chandramouli, V. V. M. S. "Dynamics of q deformed Ricker map". Journal of Difference Equations and Applications, 28(11-12), 1423-1448, 2022.

Chaotic maps have applications in diverse fields, especially in encryption [Zhang and Xiao, 2013], nonlinear control [Niu et al., 2017], watermarking [Behnia et al., 2017], data security [Li et al., 2018], etc. When existing chaotic maps are incorporated into real-time applications, researchers have identified their shortcomings in various aspects, with chaos degradation being one of the notable disadvantages. In addition, the existing chaotic maps do not have the *robust chaos*, which is defined as the nonexistence of periodic windows and coexisting attractors in the whole chaotic range. The existence of a periodic window in the chaotic range indicates that a small change in the parameter can destroy the chaos, implying frail chaos. A chaotic system with robust chaos and high sensitivity to the initial conditions can prevent chaos degradation. Thus, robust chaos is a desired property for chaos-based applications and makes the system highly complex.

The exploration of maps with high complexity has given rise to the field known as chaotification. In essence, chaotification addresses the challenge of creating new chaotic maps or developing methods to modify known maps to meet the specified properties. Since there are many chaotic maps in the literature, therefore we focus more on modifying the existing ones. The sinusoidal functions [Hua et al., 2018], exponential terms [Hua and Zhou, 2019], coupling of maps [Zhu and Wang, 2020], use of piecewise maps [Zang et al., 2021], the modulo operator [Ablay, 2022], remainder operator [Moysis et al., 2022, 2023] etc., are the popular methods of chaotification.

The Homographic Ricker map is a three-parameter flexible model capable of representing various scenarios in biological populations. However, many populations exhibit frequent changes in the ecosystem, which is not fully captured by the classical Homographic Ricker model. To address this, we propose a deformed Homographic Ricker population model obtained by applying a deformation scheme on the Homographic Ricker map $H(x)$.

In Chapter 3, we apply the deformation scheme given by Eq.(1.5) to the Homographic Ricker map (Eq. (1.4)) and obtain the q -deformed Homographic map, which is defined as

$$H_\varepsilon(x) = \frac{rx e^{-\delta x}}{(x + \beta)(1 + \varepsilon) - \varepsilon r x e^{-\delta x}}. \quad (1.8)$$

The proposed map aims to better represent the dynamics of the populations by incorporating a variable parameter (ε) that adjusts the degree of nonlinearity, enhancing the model's adaptability to rapidly changing scenarios. We discuss the dynamics of four parameter q -Homographic Ricker map (in short, q -Homographic map $H_\varepsilon(x)$) in the following parameter region

$$\widehat{\Sigma} = \left\{ (r, \beta, \delta, \varepsilon) : r > 0, \beta > 0, \delta > 0, \varepsilon > 0, \frac{r(-\beta\delta + \sqrt{\beta\delta(\beta\delta + 4)})}{\beta\delta + \sqrt{\beta\delta(\beta\delta + 4)}} e^{\beta\delta - \sqrt{\beta\delta(\beta\delta + 4)}} < 1 + \frac{1}{\varepsilon} \right\}. \quad (1.9)$$

This work focuses on the different dynamical behaviors of the q -Homographic map. The concept of the Lambert W function of rational type helps to find the upper bound for the number of fixed points, while the notion of false derivative helps to find out the specific intervals within which the fixed points of the q -Homographic map are situated. Further, we show that the deformation in the q -Homographic map leads to the positive density dependence between fitness and increased density. Moreover, we explain the chaotification of the q -Homographic map with the help of multiple remainder operator techniques, which enhances the chaotic behavior of the map. After chaotification, the map no longer exhibits the periodic behavior and coexistence of the attractors. The involved technique of chaotification introduces an additional non-linearity into the map such that it disrupts the regular behavior and promotes chaos. Lastly, we discussed the use of a feedback control approach to handle chaos in the q -Homographic map.

The above results are based on the following submitted work:

Aishwaraya and Chandramouli V.V.M.S. "Chaotification and chaos control of q -Homographic map". Submitted.

In the second part of the thesis, we examine the dynamics and investigate the nature of the prey-predator model (also known as the competition model). The analysis of the prey-predator interaction is an important field of research in non-linear dynamics. Several researchers worked on various prey-predator models ([Lotka, 1925; Volterra, 1928; Hassell and Comins, 1976; Wang and Li, 2015; Din, 2017]) because of their universal existence. The prey-predator models are the foundation of an ecosystem, and studying these models in different environments helps to keep the ecosystem stable. Another important purpose of studying these models is to predict the long-term behavior of the populations and the effects of the involved parameters.

In biology, competition is defined as the process that occurs within species that compete for limited resources to survive. The competition can be either interspecific or intra-specific. Interspecific competition is defined as the relationship of the competition for resources between organisms of the same species, and intraspecific competition refers to the competition between organisms of a different type. The competition population models gained popularity with the pioneer study of [Lotka, 1925] and [Volterra, 1928]. They independently proposed a linear two-species competition model. The proposed model is the Lotka-Volterra competition model and is the simplest and most popular example of a competition model. However, several researchers argue that the model is not helpful in predicting the behavior of complex organisms.

The prey-predator model underwent several modifications over time to incorporate reasonable assumptions to respond to changes in the environment and other factors that affect competition [Rosenzweig and MacArthur, 1963]. One of the modifications that can be introduced in any competition model is the functional response. In ecology, the functional response is the number of prey successfully attacked per predator as a function of prey density. The Holling type II functional response represents the rate of prey consumption increases with the increase in prey density, but eventually, the rate of consumption becomes constant regardless of the prey density.

Over the last three decades, researchers have turned their interest toward discrete competition models. The advantage of discrete competition models over the continuous competition model is their simplicity and applications in applied sciences. Only simple computational and graphical representation tools are enough to study the dynamical behavior of the solutions of difference equations. In many cases, the nonlinear continuous competition models do not have analytical solutions expressible in terms of finite elementary functions. This highlighted the need for a discretization scheme of continuous competition models. In [Liu and Elaydi, 2001], a discrete counterpart of the Lotka Volterra model, named as planar Ricker model, is obtained using a

non-standard discretization scheme developed by Mickens [Mickens, 1999], which is given as follows:

$$\begin{aligned}x_{n+1} &= x(n)e^{(r_1 - a_{11}x(n) - a_{12}y(n))}, \\y_{n+1} &= y(n)e^{(r_2 - a_{21}x(n) - a_{22}y(n))},\end{aligned}\tag{1.10}$$

where $x(n), y(n)$ are the competitive species, $a_{i,j}$ for $1 \leq i, j \leq 2$ are competitive parameters and r_i for $1 \leq i \leq 2$ are the carrying capacities of the competitive species x and y respectively.

Many researchers [Smith, 1998; Liu and Elaydi, 2001; Luís et al., 2011; Cabral Balreira et al., 2014; Wang and Li, 2015; Kulakov et al., 2022], have studied the planar Ricker map and explain different aspects of its dynamics. Some of them are described as follows: The conditions under which the local stability implies the global stability for the two-dimensional monotone maps are explained in [Smith, 1998]. With the help of centre manifold theory, a complete local stability analysis and bifurcation of the planar Ricker map is described in [Luís et al., 2011]. The global stability of the planar Ricker map under certain assumptions is shown in [Cabral Balreira et al., 2014] with the help of critical curves, singular points, and the preimage function.

The above research on the discrete-time competition model and the importance of the Holling type II functional response motivates to propose a 2D competition model with the Holling type II function as a per-capita birth or growth function.

In Chapter 4, we propose a generalized two-dimensional Homographic Ricker model with Holling type II function as a growth function in both the species x and y , which is defined as

$$(x_{n+1}, y_{n+1}) = \left(\left(\frac{x_n^\gamma}{x_n + \beta} \right) e^{r - x_n - ay_n}, \left(\frac{y_n^\gamma}{y_n + \beta} \right) e^{s - y_n - bx_n} \right),\tag{1.11}$$

where the parameters r, s, a, b are assumed to be positive real constants. In terms of population dynamics, the parameters r and s represent the environment's carrying capacity for species x and y , respectively, while a and b are the competition parameters. The parameter β represents the half-saturation constant of the Holling type II functional response. The existence of a Holling type II functional response and six real parameters make the dynamical analysis of the system (1.11) extremely complicated. Because of this, we limit our investigation to the specific scenario where $\gamma = 1$, and the model obtained is designated as *two-dimensional Homographic Ricker map* (in short, 2D Homographic map) is denoted by $F(x, y)$, defined as

$$F(x, y) = \left(\frac{x}{x + \beta} e^{r - x - ay}, \frac{y}{y + \beta} e^{s - y - bx} \right).\tag{1.12}$$

We analyze the dynamics of the 2D Homographic map and show that all the solutions of the map $F(x, y)$ are positive and uniformly bounded. We discuss the geometry of the 2D Homographic Ricker map with the help of critical curves and singular points. The critical curve LC_{-1} of a two-dimensional continuous map $F(x, y)$ as the collection of points for which the determinant of Jacobian of $F(x, y)$ vanishes or for which the map $F(x, y)$ is not differentiable. The critical curve LC_{-1} of a 2D Homographic map is given as follows:

$$LC_{-1} = \left\{ (x, y) \in \mathbb{R}_+^2 : y = \frac{-\beta + \sqrt{\beta^2 + \frac{4(\beta^2 - \beta x(x + \beta))}{\beta - (1 - ab)x(x + \beta)}}}{2}, x \neq \frac{-\beta + \sqrt{\beta^2 + \frac{4\beta}{1 - ab}}}{2} \right\}.\tag{1.13}$$

Whenever $ab < 1$, the critical curve LC_{-1} have the two branches LC_{-1}^1 and LC_{-1}^2 , which divided the

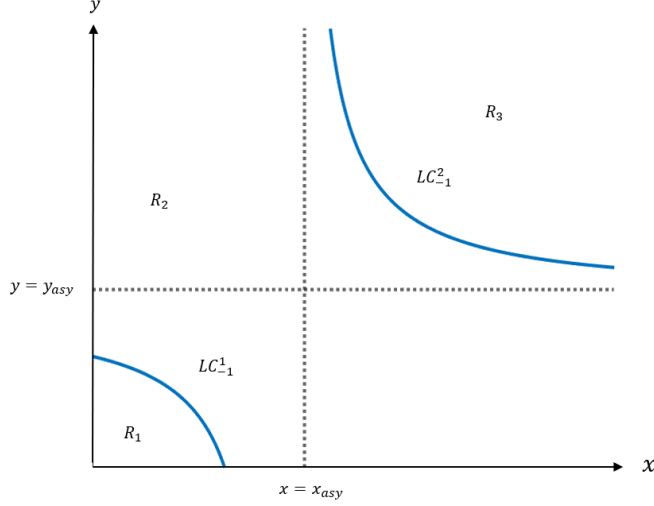


Figure 1.1 : Branches LC_{-1}^1 and LC_{-1}^2 of the critical curve LC_{-1} of the map $F(x, y)$, where

$$x_{asy} = \frac{-\beta + \sqrt{\beta^2 + \frac{4\beta}{1-ab}}}{2} \text{ and } y_{asy} = \frac{-\beta + \sqrt{\beta^2 + \frac{4\beta}{1-ab}}}{2}.$$

plane \mathbb{R}_+^2 into three regions R_1 , R_2 and R_3 as shown in Figure. 1.1, where

$$R_1 = \left\{ (x, y) \in \mathbb{R}_+^2 : y \leq \frac{-\beta + \sqrt{\beta^2 + \frac{4\beta(\beta - x(x+\beta))}{\beta - (1-ab)x(x+\beta)}}}{2} \text{ and } x < \frac{-\beta + \sqrt{\beta^2 + 4\beta}}{2} \right\},$$

$$R_3 = \left\{ (x, y) \in \mathbb{R}_+^2 : y \geq \frac{-\beta + \sqrt{\beta^2 + \frac{4\beta(\beta - x(x+\beta))}{\beta - (1-ab)x(x+\beta)}}}{2} \text{ and } x > \frac{-\beta + \sqrt{\beta^2 + \frac{4\beta}{1-ab}}}{2} \right\},$$

$$R_2 = \{\mathbb{R}_+^2 \setminus (R_1 \cup R_3)\}.$$

With the help of parametrization of the critical curve and the singular points, we obtain the following result:

Theorem 1.0.3. *Let $F(x, y)$ be the 2D Homographic map then all the points in \mathbb{R}_+^2 are either regular, fold, or cusp.*

Next, we compute the various fixed points E_0, E_1, E_2 of the map $F(x, y)$ and obtain specific conditions for the existence and uniqueness of the coexisting fixed point (x^*, y^*) . The asymptotic stability of the fixed point (x^*, y^*) is discussed, which leads to the following theorem.

Theorem 1.0.4. *The unique positive coexisting fixed point (x^*, y^*) is locally asymptotic stable if and only if*

$$|\beta(x^* + y^* + 2\beta) - (x^* + y^*)(x^* + \beta)(y^* + \beta)| < \beta^2 - \beta(x^*(x^* + \beta) + y^*(y^* + \beta)) + (1 + (1 - ab)x^*y^*)(x^* + \beta)(y^* + \beta),$$

and,

$$\beta^2 - \beta(x^*(x^* + \beta) + y^*(y^* + \beta)) < (1 + (1 - ab)x^*y^*)(x^* + \beta)(y^* + \beta).$$

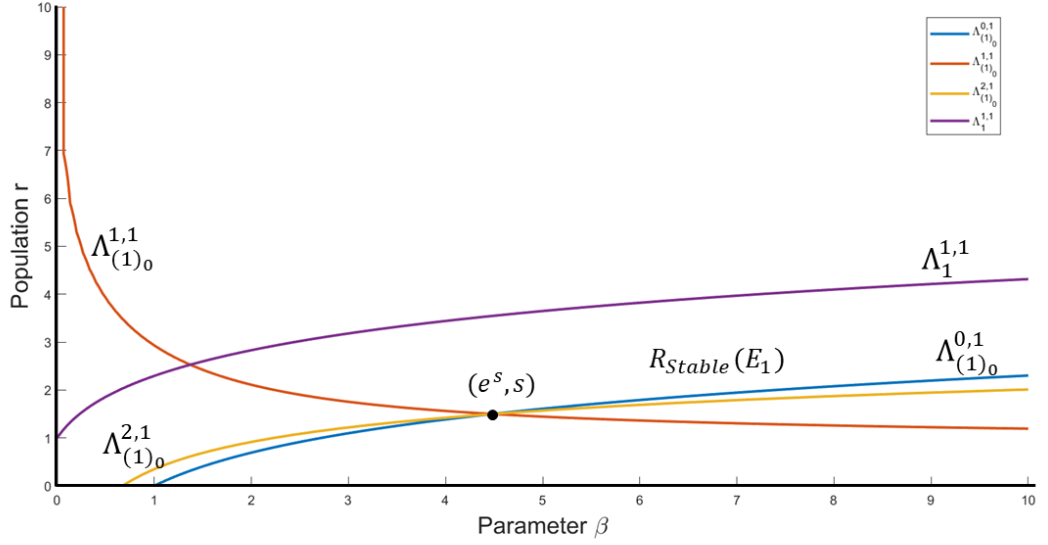


Figure 1.2 : Fold and flip bifurcation curves of the map $F(x,y)$ in the $\beta - r$ parameter plane at $s = 1.5$, $a = 0.4$, $b = 0.8$.

Further, with the help of the centre manifold theorem and bifurcation theory, we obtain the specific conditions of the existence of the flip bifurcations in the 2D Homographic map. Also, we discussed the fold and flip bifurcation curves associated with different fixed points E_0 , E_1 , E_2 of the 2D Homographic map in $\beta - r$ and $\beta - s$ parameter planes as shown in Figures 1.2 and 1.3, respectively. Let the fold and flip bifurcation curves corresponding to the fixed point E_i are denoted by $\Lambda_{(n)_0}^{i,j}$ and $\Lambda_n^{i,j}$ respectively.

Proposition 1.0.5. *Let $F(x,y)$ be the 2D Homographic map given by Eq.(1.12).*

(i) *In the $\beta - r$ parameter plane at the constant values of s , a , b , then*

$$\Lambda_{(1)_0}^{0,1} \cap \Lambda_{(1)_0}^{1,1} \cap \Lambda_{(1)_0}^{2,1} = \{(e^s, s)\}.$$

(ii) *In the $\beta - s$ parameter plane at the constant values of r , a , b , then*

$$\Lambda_{(1)_0}^{0,1} \cap \Lambda_{(1)_0}^{1,1} \cap \Lambda_{(1)_0}^{2,1} = \{(e^r, r)\}.$$

Finally, we present some numerical simulations to illustrate the theoretical results related to the stability of the positive fixed point and the bifurcation analysis w.r.t the parameter β .

The results described in chapter 4 of the thesis work are based on the following article:

Aishwaraya, and Chandramouli, V. V. M. S. "Dynamics of 2D Homographic Ricker map". Nonlinear Dynamics, 112, 3027–3053, 2023.

The classical formulation of the population model is given as

$$x_{t+1} = F(x_t),$$

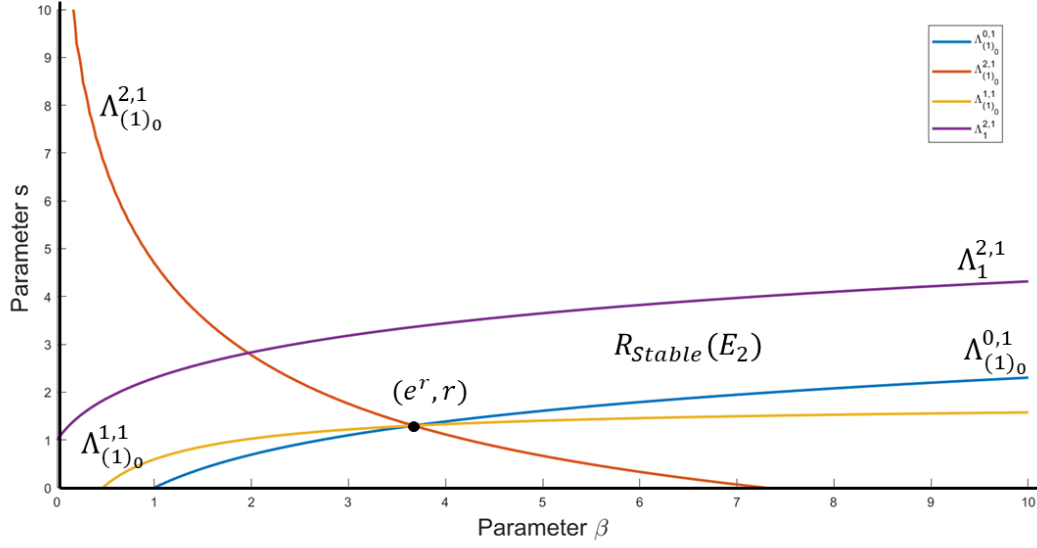


Figure 1.3 : Fold and flip bifurcation curves of the map $F(x, y)$ in the $\beta - s$ parameter plane at $r = 1.3$, $a = 0.4$, $b = 0.8$.

where F is the growth function. In the classical model, it is simply assumed that all individuals x_t at time t contribute to reproduction immediately after one time step. In other words, the newborn individuals reach sexual maturity within one breeding cycle. However, the long-lived species reach sexual maturity after several breeding cycles. To model these types of populations, the delay equations have been urged to be more appropriate. Many biological populations such as in [Papaschinopoulos and Schinas, 2012; Papaschinopoulos et al., 2014; Dilip and Mathew, 2021] have been modeled by the delayed equations to explain a more accurate representation of the population over time.

In Chapter 5, we propose a two-dimensional delayed Homographic map by introducing the delay terms in the survival functions of the 2D Homographic map, which is defined on \mathbb{R}_+^4 as follows:

$$(x_{n+1}, y_{n+1}) = \left(\alpha_1 + \frac{x_n}{x_n + \beta} e^{r-x_{n-1}-ay_{n-1}}, \alpha_2 + \frac{y_n}{y_n + \beta} e^{s-y_{n-1}-bx_{n-1}} \right), \quad (1.14)$$

where $0 < \alpha_1, \alpha_2 < 1$ and the initial conditions x_{-1} , x_0 , y_{-1} , and y_0 are arbitrary non-negative real numbers. We prove that every positive solution of the proposed model shows persistence and boundedness. Moreover, we show that the 2D delayed Homographic map admits a unique positive equilibrium, and the global convergence of the trajectories to the equilibrium point of the system (1.14) under the conditions is described as:

Theorem 1.0.6. *Suppose $A_1 < 1$, $A_2 < 1$, and $\frac{B_1 B_2}{(1-A_1)(1-A_2)} < 1$, then the system (1.14) has a unique equilibrium point $E(\bar{x}, \bar{y})$. Where $A_1 = K_1 \left(\frac{\beta + (\alpha_1 + K_1)(\alpha_1 + \beta + K_1)}{\beta^2} \right)$, $A_2 = K_2 \left(\frac{\beta + (\alpha_2 + K_2)(\alpha_2 + \beta + K_2)}{\beta^2} \right)$, $B_1 = \frac{aK_1(\alpha_1 + K_1)}{\beta}$, and $B_2 = \frac{bK_2(\alpha_2 + K_2)}{\beta}$. Also, every solution of the system (1.14) is converges to $E(\bar{x}, \bar{y})$.*

Further, we derive the criteria for the global asymptotic stability of the positive fixed point $E(\bar{x}, \bar{y})$, as mentioned in the following result:

Theorem 1.0.7. *Assume that $A_1 < 1$, $A_2 < 1$, and $\frac{B_1 B_2}{(1-A_1)(1-A_2)} < 1$, then the unique equilibrium point $E(\bar{x}, \bar{y})$ is globally asymptotically stable if the following holds true*

$$|C_1| + |C_2| + |C_1 C_2| + |(\bar{y} - \alpha_2)| + |(\bar{x} - \alpha_1)| + |C_1(\bar{y} - \alpha_2)| + |C_2(\bar{x} - \alpha_1)| + (1 - ab)|(\bar{y} - \alpha_2)(\bar{x} - \alpha_1)| < 1,$$

where $C_1 = \frac{\beta(\bar{x} - \alpha_1)}{\bar{x}(\bar{x} + \beta)}$ and $C_2 = \frac{\beta(\bar{y} - \alpha_2)}{\bar{y}(\bar{y} + \beta)}$.

The results presented above are based on the following submitted work.

Aishwaraya and Chandramouli V.V.M.S. "Dynamics of 2D delayed Homographic Ricker map". Submitted.

In the final part of the thesis, we discuss the combinatorial study of the class of symmetric bimodal maps. The simplest discrete dynamical system is the system with a unique critical point, i.e., the unimodal map. The dynamics of the unimodal map have been studied thoroughly by several researchers in different contexts [Hofbauer, 1979, 1980; Milnor and Thurston, 1988; Blokh and Lyubich, 1989; Lyubich, 1989a; Hofbauer and Keller, 1990a,b; Lyubich and Milnor, 1993; Keller and Nowicki, 1995; Pierre, 1999]. Some of them are listed as the non-existence of the asymptotic measures, some advances in the theory of unimodal maps with negative Schwarzian derivatives, and the non-existence of the wandering intervals in smooth dynamical systems with a non-degenerate critical point. Hofbauer and Keller studied the unimodal map from a combinatorial point of view in [Hofbauer, 1980; Keller, 1989, 1990] and developed tools to illustrate the kneading invariant and some geometric aspects of the unimodal maps. These tools are the Hofbauer tower and the kneading map. In [Hofbauer, 1979; Bruin, 1995], the concept of the Hofbauer tower and kneading map is used to describe the dynamics of an unimodal map symbolically. The kneading map describes the unimodal map emphasizing the recurrent behavior of the critical point and classifies its combinatorial type. The concept of the Hofbauer tower helps to picturize the unimodal map as a Markov chain with countably many states. The Hofbauer tower's geometrical interpretation illuminates the images of the central branch of the iterates of the unimodal map. The images of the central branches are essential because it leads to the concept of cutting times. The calculation of the cutting times is crucial because it helps to measure the complexity in the dynamics of unimodal maps [Bruin, 1999].

Recently, the discrete dynamical system has turned its attention to the bimodal maps with relatively complete knowledge of the dynamics and topological entropy of the unimodal maps. The bimodal maps and their importance have been highlighted during the study of the dynamics of degree one circle maps [Fournier-Prunaret, 1987; De Melo and Van Strien, 1989]. The presence of bistable cycles in the bimodal maps makes their dynamical behavior more interesting than that of unimodal maps. The dynamics and bifurcations of the family of bimodal maps have been discussed by many authors [Mackay and Tresser, 1987; Ringland and Schell, 1991; Milnor, 1992; Ringland and Tresser, 1995; Lofaro, 1997b]. The dynamics of the symmetric bimodal maps were discussed by Gumowski and Mira [Gumowski and Mira, 1980] and Chavoya-Aceves et al. [Chavoya-Aceves et al., 1985]. The bifurcation analysis and various properties of the symmetric odd bimodal map have been discussed in [Lofaro, 1997a,b]. Further, the topological properties of the Fibonacci bimodal map in the context of the kneading map are discussed in [Ji and Ma, 2023]. It also showed that a phase transition occurs from Lebesgue conservative to Lebesgue dissipative behavior. However, in [Vargas, 2008], the Fibonacci bimodal map is constructed with the help of the natural symmetry of a bimodal map using a twin principle nest.

In Chapter 6, we extend two important combinatorial tools of the unimodal maps, i.e., the Hofbauer tower and the kneading map, for a class of symmetric bimodal maps \mathcal{F} .

Before proceeding further, we recall some basic definitions and concepts.

Let I be a compact interval $[a, b] \subset \mathbb{R}$. Suppose $f: I \rightarrow I$ be a continuous piecewise monotone map; then such a map f is called a *bimodal map*, if it has two local extrema points in (a, b) . Assume that c^+ and c^- are the points of local extrema and f is strictly monotone in each of the three intervals.

Let

$$I_1 = [a, c^+); I_2 = (c^+, c^-); I_3 = (c^-, b].$$

A map f is said to be a bimodal map of type $(+ - +)$ if $f'(x) > 0$ for $x \in I_i$, where $i = 1, 3$ and $f'(x) < 0$ for $x \in I_i$, $i = 2$.

The Hofbauer tower \hat{I} for the bimodal map f is the union of I^+ and I^- , where I^+ and I^- are the Hofbauer tower corresponding to the critical points c^+ and c^- respectively, i.e.,

$$\hat{I} = I^+ \cup I^-.$$

The tower I^+ and I^- are the disjoint union of the intervals $D_n^+ \in I$ and $D_n^- \in I$ respectively, such that

$$I^+ = \sqcup D_n^+ \text{ and } I^- = \sqcup D_n^-.$$

Let $D_1^+ = (c_1^+, c_1^-)$, and $D_2^+ = (c_2^+, c_1^-)$. For $n \geq 3$, the levels of positive Hofbauer tower I^+ are defined inductively as:

$$D_{n+1}^+ = \begin{cases} f(D_n^+) & \text{if } c^+, c^- \notin cl(D_n^+) \\ (c_{n+1}^+, c_1^+) & \text{if } c^+ \in cl(D_n^+) \\ (c_{n+1}^+, c_1^-) & \text{if } c^- \in cl(D_n^+) \\ (c_{n+1}^+, c_1^{\otimes}) & \text{if } c^+, c^- \in cl(D_n^+), \end{cases} \quad (1.15)$$

where $\otimes \in \{+, -\}$ and c_n^+, c_n^- , are the forward images of the critical points c^+, c^- , respectively.

$$c_1^{\otimes} = \begin{cases} c_1^- & \text{if } c_n^+ > c^- \\ c_1^+ & \text{if } c_n^+ < c^+. \end{cases}$$

If any case of Eq.(1.15) applies except the first case, then n is called the cutting time of positive Hofbauer tower I^+ and it is denoted by ${}^+S_k$. Corresponding to the positive Hofbauer tower, we have three types of cutting times, i.e., positive, negative, and double cutting time. The negative Hofbauer tower I^- and its associated cutting time can be defined similarly. Since the bimodal map f is symmetric, the cutting time associated with the positive and negative Hofbauer tower are the same and denoted by S_k^* . The difference of two consecutive cutting times gives the following result.

Lemma 1.0.8. *Let $f \in \mathcal{F}$ be a bimodal map and S_k^* be the cutting time of f . Then $S_k^* - S_{k-1}^* = S_m^*$ for some $m < k - 1$, i.e., the difference of two subsequent cutting times is again a cutting time.*

The above Lemma leads to the definition of the *kneading map* Q , where $Q: \mathbb{N} \rightarrow \mathbb{N} \cup \{\infty\}$ such that

$$S_{Q(k)}^* = S_k^* - S_{k-1}^*. \quad (1.16)$$

In order to make things complete, let $Q(0) = 0$. If S_k^* does not exist then we consider $S_k^* = \infty$, in this case $Q(k) = \infty$. The kneading map of the symmetric bimodal map $f(x)$ satisfies the following:

Proposition 1.0.9. *Let $f(x) \in \mathcal{F}$ and satisfies the condition $f(c^-) \geq -z$. The kneading map Q is an admissible kneading map if and only if*

$$\{Q(k+j)\}_{j \geq 1} \succeq \{Q(Q^2(k)+j)\}_{j \geq 1}$$

for all $k \geq 1$. Here, \succeq denotes the lexicographical order.

We also give extensions of these combinatorial tools, namely, the extended Hofbauer tower, the co-kneading map $\tilde{Q}(k)$, and the co-cutting time \tilde{S}_k^* . The extended tools illustrate the recurrence behavior of the critical points, which are not clearly visible in the kneading map and the Hofbauer tower. The result on the co-cutting times is obtain as follows:

Proposition 1.0.10. *Let $f \in \mathcal{F}$ be a bimodal map and \tilde{S}_k^* be the co-cutting time of f . Then $\tilde{S}_k^* - \tilde{S}_{k-1}^* = S_m^*$ for some m , i.e., the difference of two subsequent co-cutting times is a cutting time.*

Further, we propose an algorithm to compute the variety of cutting times with the help of kneading invariants associated with the critical points. Finally, we discuss the geometric interpretation of the Hofbauer tower and its extended version. Also, we explore the notion of splitting of the kneading invariants associated with two critical points of the symmetric bimodal maps. The splitting of the kneading invariant indicates the combinatorial definition of the kneading map, and it helps to explain the admissibility conditions.

The above results are based on the following submitted work:

Aishwaraya, and Chandramouli, V.V.M.S. "Combinatorics of symmetric bimodal maps". Submitted.

